Research Article | Vol. 15, No. 4 / 1 Apr 2024 / Biomedical Optics Express 2517

Biomedical Optics EXPRESS

Effects of intraocular scatter on near peripheral vision

AUGUSTO ARIAS, DIEGO MONTAGUD-MARTINEZ, AND PABLO ARTAL*

Laboratorio de Óptica, Centro de Investigación en Óptica y Nanofísica (CiOyN), Universidad de Murcia, Campus de Espinardo (Ed. 34), 30010 Murcia, Spain
pablo@um.es

Abstract: Both cataracts and age-related macular degeneration (AMD) may occur with aging and are often developed simultaneously. We performed a study to better characterize the impact of induced scatter on the quality of vision in the near periphery, a region where individuals with AMD typically maintain their functional vision. We used an optical instrument as a cataract simulator based on projecting at the eye's pupil plane phase masks with controlled spatial properties generated with a spatial light modulator. The phase wavefronts were designed to accurately replicate the angular distribution of light intensity in the retina found in cataractous eyes with different severities. The induced amount of scatter ranged from values of straylight (S) from 10 to 85 degree^2/sr, which corresponds from normal aging eye to advanced cataract stages. Mesopic visual acuity (VA) and contrast sensitivity (CS) at 3 cycles per degree were measured at the fovea and two retinal eccentricities (5 and 10 degrees in nasal visual field). We observed a consistent linear decline in VA (expressed in LogMAR) as the amount of induced scatter (quantified by the straylight parameter S) increased, both at the fovea and in the periphery. The effect of induced scattering on mesopic VA and CS at the fovea and the near periphery was evaluated. We found a relatively lower impact of scatter in the near periphery. This may explain the modest improvement in vision often found after cataract surgery in patients with AMD.

1. Introduction

Cataracts represent a prevalent ocular pathology characterized by increased light scattering, often referred to as straylight, due to lens opacification. The visual impact of cataracts manifests as both image blurring and reduced contrast. Conversely, age-related macular degeneration (AMD) is a retinal disorder leading to the loss of central foveal vision, forcing patients to rely on peripheral vision, where cone density is lower. Both of these pathologies are frequently associated with the aging process and can co-occur. While cataracts can be effectively addressed through widely practiced cataract surgery, the extent of their benefits can be constrained by concomitant ocular comorbidities [1], such as AMD [2–6].

Intraocular scatter in cataract patients is related with the extension of their point-spread function (PSF) and is often characterized by the straylight parameter (S). In prior psychophysical experiments, artificial intraocular-like scattering has commonly been induced using filters initially designed for professional photography or employed in treatments for amblyopia and strabismus [7–12]. These filters generate levels of scattered light akin to those observed in cataract-affected eyes at specific angles. However, it's important to note that the angular distribution of their scattered light doesn't align with the expected distribution for a standard observer [13], as defined by the International Commission on Illumination (CIE) [14]. In our previous research [15], we demonstrated that intraocular scattering can be accurately replicated using random phase perturbations. In the present study, we have adopted this approach to artificially induce controlled amounts of intraocular straylight by displaying random phase maps on a spatial light modulator (SLM). Our study aims to gain deeper insights into the benefits of cataract surgery for patients

#523715 https://doi.org/10.1364/BOE.523715
Journal © 2024 Received 13 Mar 2024; accepted 14 Mar 2024; published 19 Mar 2024

Biomedical Optics EXPRESS

with AMD. To achieve this, we conducted an assessment of Visual Acuity (VA) and Contrast Sensitivity (CS) – at a single spatial frequency – at three distinct retinal locations: the fovea and two eccentricities within the nasal visual field. We employed a cataract-visual simulator for these evaluations. These eccentricities were selected to correspond to different AMD grades, representing retinal areas that still retain functional vision. We establish relationships between the visual metrics and the level of straylight.

2. Methods

2.1. Experimental apparatus

We adapted a previously constructed instrument designed for the production and measurement of programmable amounts of straylight [15] to serve as a visual simulator, as illustrated in Fig. 1(a). In this instrument, a liquid crystal Spatial Light Modulator (SLM) (model PLUTO, Holoeye, Germany) is employed to introduce random phase maps to the wavefront of light emitted from a monitor. An 8 mm circular aperture was adjusted to the SLM. Optical conjugation between the SLM and the eye's pupil was achieved by using a telescope (formed by the lenses L1 and L2 in Fig. 1(a)) with a magnification factor of 1/6, thereby expanding the angular range of the Point Spread Function (PSF) to a maximum of 11.9 degrees. Additionally, this magnification effectively reduced the pupil's size projected onto the eye to 1.33 mm, mitigating aberrations originating from both the SLM and the eye. The telescope also incorporated a linear polarizer and a green spectral filter (central wavelength: 540 ± 10 nm). These components were employed to minimize non-diffracted light and chromatic aberrations originating from the SLM, respectively. The stimuli maintained an approximate mean luminance of ~0.3 cd/m^2, a result of light diffraction by the pixelated SLM's structure and spectral filtering within the visual simulator. The luminance was measured using a CMOS camera (DCC1545 M; Thorlabs Inc., Germany) previously calibrated with a luminance meter (LS-100; Konica-Minolta Inc, Japan).

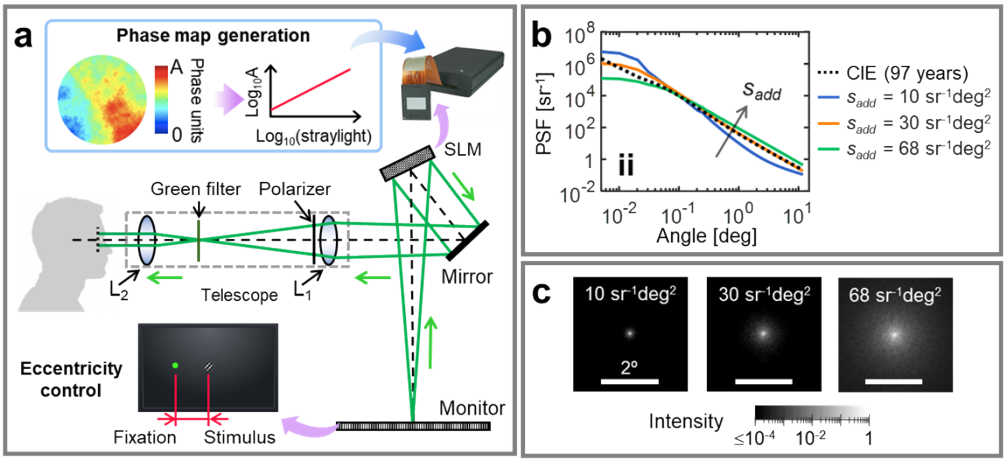

Fig. 1. Generation of artificial intraocular straylight. a) instrument with a spatial light modulator (SLM) where random phase maps are displayed to induce the straylight. Several amounts of straylight are programmed via the phase map amplitude (A). The focal lengths of lenses L1 and L2 are 150 and 25 mm, respectively. b) Examples of radial profiles of the generated PSFs adding different amounts of straylight (s_add) at 6°, compared with the PSF_{CIE} for a 97 years old standard eye. c) Examples of PSF images that add the labeled amounts of straylight.

Biomedical Optics EXPRESS

The methodology for generating programmable levels of straylight through random phase perturbations is detailed in a separate publication [15]. In essence, we compute a pseudo-self-replicant surface whose discrete cosine spectrum is modulated by a power-law function. The parameters of this function were optimized through numerical methods to replicate the PSF of a standard observer, as defined by the International Commission on Illumination (CIE) through the following equation:

$$PSF_{CIE}(\theta) = \left[1 - 0.08\left(\frac{A}{70}\right)^4\right]\left[\frac{9.2\times10^6}{\left[1+(\theta/0.0046)^2\right]^{1.5}} + \frac{1.5\times10^5}{\left[1+(\theta/0.045)^2\right]^{1.5}}\right] + \left[1 - 1.6\left(\frac{A}{70}\right)^4\right]\left\{\left[\frac{400}{1+(\theta/0.1)^2} + 3\times10^{-8}\theta^2\right] + p\left[\frac{1300}{\left[1+(\theta/0.1)^2\right]^{1.5}} + \frac{0.8}{\left[1+(\theta/0.1)^2\right]^{0.5}}\right]\right\} + 2.5\times10^{-3}p \quad (1)$$

where θ is the retinal angle (in degrees), A is the age and p is the pigmentation factor. p was set to 1, representing light eyes.

Subsequently, various degrees of straylight can be generated by adjusting the amplitude of the calculated phase map, leveraging their linear relationship (refer to the inset in Fig. 1(a)). Intraocular scattering is quantified by the straylight parameter (s), calculated as:

$$s = \theta^2 \times PSF(\theta) \quad (2)$$

where PSF(θ) is the point-spread-function as a function of θ.

Figure 1(b) presents the PSFs measured from the phase maps employed for the generation of the additions intraocular straylight (s_add) at a 6-degree angle, computed using Eq. (2). These PSF profiles were retrieved using images acquired with an electron-multiplying CCD camera (Luca; Andor, UK) for angles less than 0.25° (see examples in Fig. 1(c)), and the optical integration method [16] for angles larger than or equals to 0.25°. Figure 1(b) also provides a comparison between experimentally retrieved PSFs adding different amounts of straylight and the CIE-defined PSFs, illustrating their good agreement (particularly for angles larger than 0.1°). It was observed that the baseline level of straylight (i.e., when displaying a flat phase map on the SLM) measures 10.2 deg^2sr^{-1}. This inherent offset is primarily attributed to the presence of the nematic liquid crystal within the SLM [17]. Figure 1(c) shows examples of the generated PSF images.

2.2. Visual testing

For VA assessments, subjects were presented with a tumbling E displayed on the monitor in white-on-black. The size of the optotype (range, 1.3 to 100 arcmin) was systematically reduced until the subject consistently failed in three or more out of five randomly oriented trials. Subsequently, VA was quantified in LogMAR units, calculated as the logarithm of the angular resolution in minutes of arc (arcmin). The angular resolution was determined as one-fifth of the size of the smallest optotype for which the subject correctly identified more than two trials. VA assessments were conducted at the fovea and two peripheral locations (5 and 10 degrees in the nasal visual field) while introducing intraocular straylight levels ranging from 10.2 to 82.4 deg^2sr^{-1}. For foveal VA, we expanded the range of straylight increments compared to peripheral measurements to explore their relationship. During peripheral VA measurements, an LED served as a fixation point on the monitor. Ten subjects, with an average age of 30 years (±4 years) and refractive errors within 0.75D for defocus and astigmatism, who did not have any ocular pathology, were recruited as participants for this experiment.

Biomedical Optics EXPRESS

Similar to the VA assessments, CS testing was conducted at the fovea as well as two peripheral locations (5 and 10 degrees) within the nasal visual field. For this evaluation, the stimulus utilized was a Gaussian-windowed sinusoidal grating with a spatial frequency of 3 cycles per degree (cpd), as lower spatial frequencies are particularly sensitive to the effects of cataracts [18]. Subjects were asked to identify the orientation of the grating, choosing between two randomly presented options: left (45°) or right (135°). In each trial, the stimulus was displayed on the monitor for 300 ms following an auditory cue, with the grating's contrast determined using a QUEST algorithm. The CS was subsequently reported based on the results of 50 trials conducted for each eccentricity. Initially, the relationship between foveal CS and the degree of induced straylight was explored in three subjects without any ocular pathology and also nearly emmetropes (within 0.75D), who were of similar age (30 ± 1 years). This investigation involved measuring CS while introducing four levels of straylight additions, ranging from 10.2 to 39.1 deg^2sr^{-1}. These measurements were repeated twice. Subsequently, CS was assessed in a different set of five emmetropic subjects (age, 34 ± 12 years;) using three levels of straylight additions (10.2, 29.4, and 58.3 deg^2sr^{-1}) at the fovea and two eccentricities within the nasal visual field.

All measurements were performed under natural viewing conditions, that is, accommodation was not paralyzed and the pupil was not dilated. All VA and CS measurements were conducted in a dark room. The study followed the tenets of the Declaration of Helsinki, and signed informed consent was obtained from the subjects after the nature and all possible consequences of the study had been explained. The study was approved by the Ethics commission of the University of Murcia. All measurements were exclusively carried out on their dominant eyes, being determined by the "Hole-in-the-hand" test. The use of a small artificial pupil minimized the impact of their natural aberrations; nevertheless, any remaining spherical refractive errors were individually corrected for each subject. To achieve this correction, subjects were given the ability to remotely adjust the amplitude of spherical wavefronts projected onto the SLM until the optotype was clearly focused at the fovea.

3. Results

Figure 2(a) depicts the relationship between VA and the increment in straylight (s_add) at three distinct eccentricities. The linear regression analysis of VA in LogMAR units against s_add is primarily based on the foveal measurements, where s_add values are elevated. The influence of s_add on VA diminishes as eccentricity increases, as evidenced by the varying slopes in the linear fits. This trend is further illustrated in Fig. 2(b), which illustrates VA as a function of eccentricity.

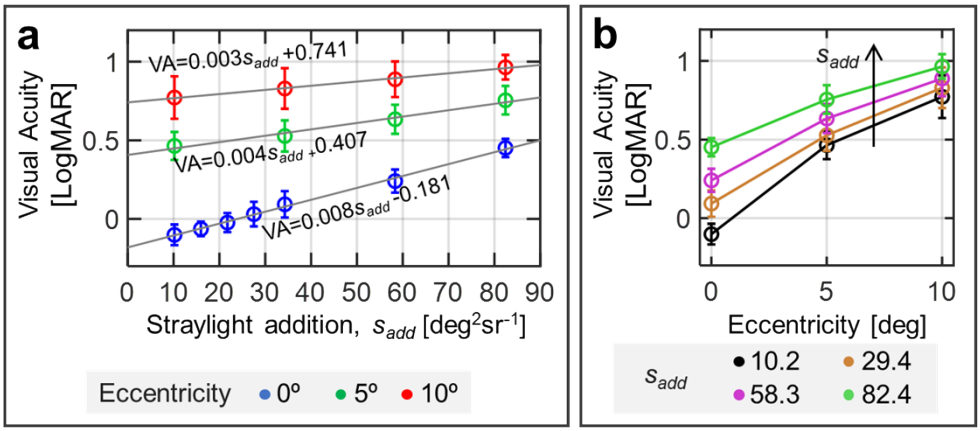

Fig. 2. Mean VA as a function of: a) the additions of straylight s_add with linear fittings and b) the eccentricity. In a), bars represent standard deviation.

Biomedical Optics EXPRESS

Figure 3(a) presents the logarithmic foveal CS as a function of s_add. The observed relationship between these two parameters is linear, as supported by high Pearson coefficients ($r^2 > 0.9654$). A similar linear fitting approach was applied to measurements at various eccentricities, as illustrated in Fig. 3(b). The logarithmic CS data from Fig. 3(b) is further visualized in Fig. 3(c), this time as a function of retinal eccentricity.

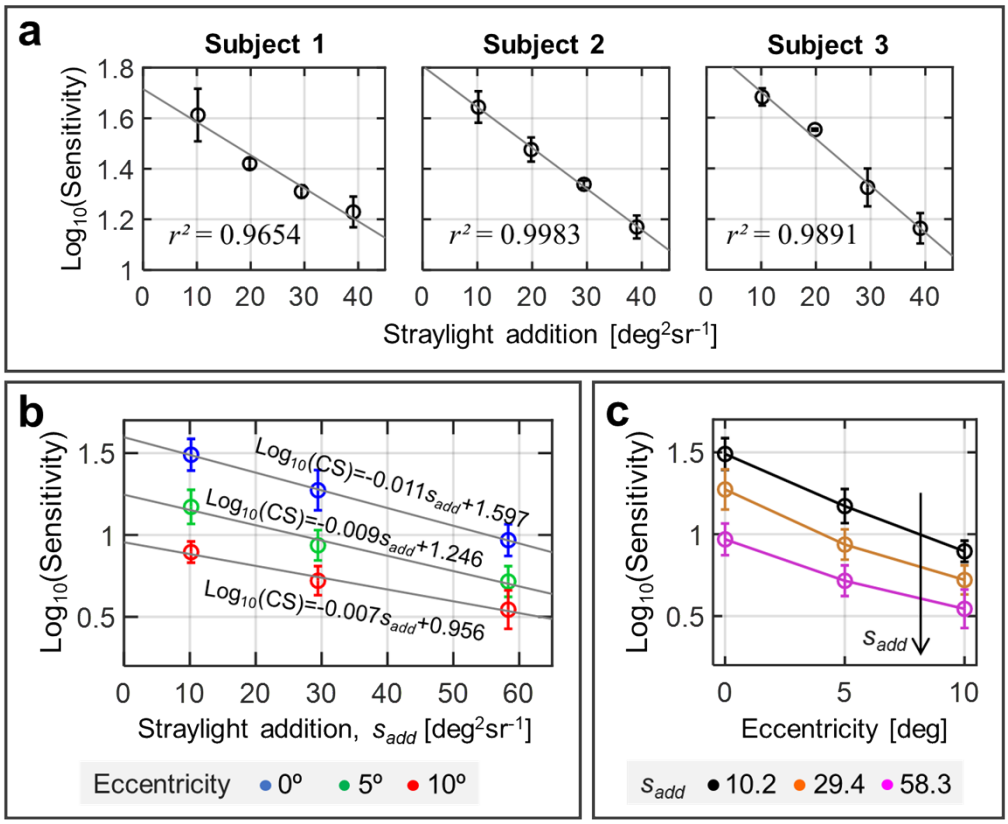

Fig. 3. Eccentricity and straylight dependence of the CS at 3 cycles per degree. a) Mean of foveal CS in three subjects as a function of the straylight addition (s_add). b) Mean and standard deviation (point and bars, respectively) of CS in five subjects as a function of the addition of straylight. c) Mean of CS as a function of the eccentricity. Unit of s_add in c) are deg2sr-1.

4. Discussion and conclusions

In this study, we examined the combined effects of increased intraocular scattering and retinal eccentricity in the nasal visual field on both Visual Acuity (VA) and Contrast Sensitivity (CS). To accomplish this, we developed a visual simulator based on spatial light modulation, capable of replicating the levels and angular distribution of intraocular straylight in accordance with the standards defined by the International Commission on Illumination (CIE). Our simulator mimics the maximum levels and angular distributions of straylight found in eyes graded 2 (~29 deg^2sr^{-1}) and 3 (~62 deg^2sr^{-1}) on the LCOS-III system [19], which are characteristic of cataractous eyes.

As anticipated, our findings reveal that visual quality deteriorates with both eccentricity and increasing straylight. However, our results highlight several key observations: i. both VA (in logMAR units) and logarithmic CS exhibit a linear dependence on the added amounts of

Biomedical Optics EXPRESS

straylight; ii. a decrease in the impact of straylight on VA and CS as eccentricity decreases; and iii. a greater influence of eccentricity on VA compared to CS. These findings offer insights that may help to elucidate the limited improvements in vision often observed in AMD patients following cataract surgery [2–6]. In particular, the magnitude of change in VA between the highest and lowest levels of added straylight becomes less pronounced as the stimulus eccentricity increases (refer to Fig. 2). In this study, the amounts of straylight are associated with representations of cataractous eyes (where internal ocular aberrations are generally increased) and, therefore, correlate with reductions in visual acuity. Nevertheless, the fidelity of those representations and the VA dependence relies on the morphology of cataracts, being more accurate for nuclear cataracts. This is because increased amounts of scattered light don't generally imply a reduction in VA. While VA changes stem from the redistribution of light within a narrow angular domain ($<1°$, approximately) of the PSF due to aberrations (i.e., phase maps of low spatial frequency), scattering alters the light distribution across larger angles of the PSF.

It is important to note that a direct comparison of our results with published clinical results on the impact of cataract surgery in AMD patients is challenging due to the absence of objective AMD scores or variations in cataract scoring systems (e.g., LOCS-III, objective scatter index (OSI), and Log(s)). Additionally, three experimental factors may contribute to disparities between our VA and CS measurements and those reported in studies exploring the effects of straylight or eccentricity on visual quality. First, the relatively low luminance of our stimuli (approximately 0.3 cd/m^2) within the visual simulator led to measured visual outcomes (both VA and CS) that are generally lower than those observed in clinical assessments [20,21].This is the main reason for the difference between our measured and reported [22] peripheral CS values when no straylight was added. A possible ways to overcome this issue is the incorporation of a brighter monitor or a digital light projector. Second, the artificial pupil size used in our measurements was only 1.33 mm in diameter, which is smaller than the expected pupil sizes for elderly individuals (>3.7 mm with a luminance lower than 1 cd/m^2 [23]). This difference impacts VA values, as a smaller pupil size reduces the influence of low- and high-order aberrations, which are typically larger in cataract-affected eyes [24]. We do not anticipate that this difference significantly affects CS measurements since CS at low spatial frequencies is less susceptible to aberrations. It is well-documented that straylight reduces CS values across all spatial frequencies [9,25]. Third, projecting quasi-monochromatic stimuli, as done in our study, is not common in clinical practice. However, this quasi-monochromatic was necessary to ensures fidelity in reproducing the programmed scattering effects, as the phase modulation of the SLM depends on the wavelength. Lastly, it is worth noting that our study did not account for adaptation to straylight, as stimuli were presented for very brief durations (<1s).

In summary, we conducted measurements of mesopic VA and CS at the fovea and within the nasal visual field while incrementally introducing intraocular straylight. The found dependencies of VA and CS with the eccentricity and additions of straylight allow us to better explain the clinical outcomes of cataract surgery in AMD patients.

Funding. Agencia Estatal de Investigación (PID2019-105684RB-I00/AEI/10.13039/501100011033).

Disclosures. The authors do not have any disclosure to declare.

Data availability. Data underlying the results presented in this paper are not publicly available, but it may be obtained from the corresponding author upon reasonable request.

References

1. M. Lundström, U. Stenevi, and W. Thorburn, "Outcome of cataract surgery considering the preoperative situation: a study of possible predictors of the functional outcome," Br. J. Ophthalmol. **83**(11), 1272–1276 (1999).
2. F. Forooghian, E. Agrón, T. E. Clemons, *et al.*, and Age-Related Eye Disease Study Research Group, "Visual acuity outcomes after cataract surgery in patients with age-related macular degeneration: age-related eye disease study report no. 27," Ophthalmology **116**(11), 2093–2100 (2009).
3. M. Lundström, K. G. Brege, I. Florén, *et al.*, "Cataract surgery and quality of life in patients with age related macular degeneration," Br. J. Ophthalmol. **86**(12), 1330–1335 (2002).

Biomedical Optics EXPRESS

4. Y. Ma, J. Huang, B. Zhu, *et al.*, "Cataract surgery in patients with bilateral advanced age-related macular degeneration: Measurement of visual acuity and quality of life," J. Cataract Refract. Surg. **41**(6), 1248–1255 (2015).
5. E. Mönestam and B. Lundqvist, "Long-term visual outcome after cataract surgery: Comparison of healthy eyes and eyes with age-related macular degeneration," J. Cataract Refract. Surg. **38**(3), 409–414 (2012).
6. M. Vianya-Estopa, W. A. Douthwaite, C. L. Funnell, *et al.*, "Clinician versus potential acuity test predictions of visual outcome after cataract surgery," Optom. - J. Am. Optom. Assoc. **80**(8), 447–453 (2009).
7. F. Martino, S. Ortiz-Peregrina, J. J. Castro-Torres, *et al.*, "Visual performance after the deterioration of retinal image quality: induced forward scattering using Bangerter foils and fog filters," Biomed. Opt. Express **12**(5), 2902–2918 (2021).
8. H. Ginis, P. Artal, A. Pennos, *et al.*, "Performance of a differential contrast sensitivity method to measure intraocular scattering," Biomed. Opt. Express **8**(3), 1382–1389 (2017).
9. E. M. Colombo and C. Paz-Filgueira, "Quantifying the effect of straylight on photopic contrast sensitivity," J. Opt. Soc. Am. A **35**(7), 1124–1130 (2018).
10. R. S. Anderson, T. Redmond, D. Rodney McDowell, *et al.*, "The robustness of various forms of perimetry to different levels of induced intraocular stray light," Invest. Ophthalmol. Vis. Sci. **50**(8), 4022–4028 (2009).
11. J. Pujol, M. Vilaseca, E. M. Colombo, *et al.*, "Comparison between an objective and a psychophysical method for the evaluation of intraocular light scattering," J. Opt. Soc. Am. A **29**(7), 1293–1299 (2012).
12. M. B. Zlatkova, E. E. Coulter, and R. S. Anderson, "The effect of simulated lens yellowing and opacification on blue-on-yellow acuity and contrast sensitivity," Vision Res. **46**(15), 2432–2442 (2006).
13. G. C. De Wit, L. Franssen, J. E. Coppens, *et al.*, "Simulating the straylight effects of cataracts," J. Cataract Refract. Surg. **32**(2), 294–300 (2006).
14. J. J. Vos, B. L. Cole, H.-W. Bodmann, *et al.*, *CIE Equations for Disability Glare* (CIE Collection, 2002), pp. 1–9.
15. A. Arias, H. Ginis, and P. Artal, "Light scattering in the human eye modelled as random phase perturbations," Biomed. Opt. Express **9**(6), 2664 (2018).
16. H. Ginis, G. M. Perez, J. M. Bueno, *et al.*, "The wide-angle point spread function of the human eye reconstructed by a new optical method," J. Vis. **12**(3), 20 (2012).
17. M. H. Kao, K. A. Jester, A. G. Yodh, *et al.*, "Observation of light diffusion and correlation transport in nematic liquid crystals," Phys. Rev. Lett. **77**(11), 2233–2236 (1996).
18. N. A. P. Brown, "The morphology of cataract and visual performance," Eye **7**(1), 63–67 (1993).
19. O. Sahin, A. Pennos, H. Ginis, *et al.*, "Optical measurement of straylight in eyes with cataract," J. Refract. Surg. **32**(12), 846–850 (2016).
20. C. Schwarz, S. Manzanera, and P. Artal, "Binocular visual performance with aberration correction as a function of light level," J. Vis. **14**(14), 6 (2014).
21. S. T. L. Chung and G. E. Legge, "Comparing the shape of contrast sensitivity functions for normal and low vision," Invest. Ophthalmol. Vis. Sci. **57**(1), 198–207 (2016).
22. J. Rovamo, V. Virsu, and R. Nasanen, "Cortical magnification factor predicts the photopic contrast sensitivity of peripheral vision," Nature **271**(5640), 54–56 (1978).
23. H. H. Telek, H. Erdol, and A. Turk, "The effects of age on pupil diameter at different light amplitudes," Beyoglu Eye J. **3**, 80–85 (2018).
24. T. Fujikado, T. Kuroda, N. Maeda, *et al.*, "Light scattering and optical aberrations as objective parameters to predict visual deterioration in eyes with cataracts," J. Cataract Refract. Surg. **30**(6), 1198–1208 (2004).
25. T. J. T. P. van den Berg, L. Franssen, and J. E. Coppens, "Ocular media clarity and straylight," in *Encyclopedia of the Eye* (Elsevier/Academic Press, 2010), pp. 173–183.